UNIVERSITI PUTRA MALAYSIA

EVALUATION OF MICROMORPHOLOGICAL CHANGES IN LATERAL AND MEDIAL CONDYLE OF THE FEMUR AND TIBIA IN BOTH SURGICALLY AND CHEMICALLY INDUCED OSTEOARTHRITIC KNEE IN A RABBIT MODEL

YEE XUE ROU

Ip
FPV 2020 61

EVALUATION OF MICROMORPHOLOGICAL CHANGES IN LATERAL AND MEDIAL CONDYLE OF THE FEMUR AND TIBIA IN BOTH SURGICALLY AND CHEMICALLY INDUCED OSTEOARTHRITIC KNEE IN A RABBIT MODEL

YEE XUE ROU

A project paper submitted to the
Faculty of Veterinary Medicine, Universiti Putra Malaysia
In partial fulfillment of the requirement for the
DEGREE OF DOCTOR OF VETERINARY MEDICINE
Universiti Putra Malaysia
Serdang, Selangor Darul Ehsan

2020/2021

It is hereby certified that I have read this project paper entitled "Evaluation of Micromorphological Changes in Lateral and Medial Condyle of the Femur and Tibia in Both Surgically and Chemically Induced Osteoarthritic Knee in a Rabbit Model", by Yee Xue Rou and in my opinion it is satisfactory in terms of scope, quality, and presentation as partial fulfillment of the requirement for the course VPD 4999 – Final Year Project.

Assoc Prof Dr. Lau Seng Fung

DVM (UPM), PhD (UTRECHT)

Senior Lecturer,

Faculty of Veterinary Medicine

Universiti Putra Malaysia

(Supervisor)

ACKNOWLEDGEMENTS

First of all, I would like to express my special thanks of gratitude to Associate Professor Dr. Lau Seng Fong who given me this golden opportunity and guidance to complete my final year project with the topic of Evaluation of Micromorphological Changes of the Lateral and Medial Condyle of the Femur in Both Surgically and Chemically Induced Osteoarthritic Knee in a Rabbit Model. Thanks to Dr. Lau, I had learnt a lot of new knowledges about osteoarthritis and micro-CT which I had never encounter before.

Secondly, I really thankful to both of my parents and friends who gives moral support and accompany me going through the process. Thanks to my friends for giving me suggestions and helping me a lot with this project.

CONTENTS

LIST OF TABLES

LIST OF FIGURES

ABBREVIATIONS

2-D	Two dimensional
3-D	Three dimensional
ACLT	Anterior cruciate ligament transection
ANOVA	Analysis of variance
BS/TV	Bone surface density
BV	Bone volume
BV/TV	Bone to tissue volume
IACUC	Institutional Animal Care and Use Committee
MIA	Monosodium iodoacetate
Micro-CT	Micro-computed tomography
OA	Osteoarthritis
OARSI	Osteoarthritis Research Society International
PTOA	Post traumatic osteoarthritis
Q1	First quartile
Q3	Third quartile
ROI	Regions of interest
Tb.N	Trabecular number
Tb.Sp	Trabecular separation
Tb.Th	Trabecular thickness
TV	Tissue volume
YLD	Year lived with disability

Abstrak daripada kertas projek yang dikemukakan kepada Fakulti Perubatan Veterinar untuk memenuhi sebahagian daripada keperluan kursus VPD4999 – Projek Ilmiah Tahun Akhir.

PENILAIAN PERUBAHAN MIKROMORFOLOGI TULANG SUBKONDRAL DI MEDIAL DAN LATERAL CONDYLE FEMUR DENGAN MENGGUNAKAN KIMIA AND SURGIKAL UNTUK MENYEBABKAN OSTEOARTRITIS DI SENDI LUTUT ARNAB

Oleh

YEE XUE ROU

No. Matrik : 188519

Penyelia : Associate Professor Dr. Lau Seng Fong

ABSTRAK

Osteoarthritis ialah sejenis arthritis disebabkan oleh inflamasi, kerosakan dan kehilangan tulang rawan di sendi. Diagnosis osteoarthritis di stage awal masih tidak jelas kerana pathogenesis penyakit ini sangat rumit. Kajian terhad yang mengenai perbezaan perubahan antara medial dan lateral condyle di lutut semasa osteoarthritis. Oleh itu, kajian ini dilaksanakan. Objektif kajian ini adalah untuk mengesan dan menilai perubahan mikromorfologi tulang subkondral di osteoarthritik medial dan lateral condyle lutut seperti peratusan jumlah tulang trabecular (BV/TV), permukaan

tulang/ permukaan tisu (BS/TV), ketebalan trabecular (Tb.Th) dan ketebalan plat (Tb.Sp) di osteoarthritis yang disebabkan oleh kimia and surgikal dari masa yang berbeza (Minggu ke-4, ke-8 dan ke-12). Tiga puluh lima arnab baka *New Zealand White* (n=35) telah dibahagikan kepada tiga kumpulan: kumpulan kontrol (n=5), kumpulan MIA (n=15) dan kumpulan ACLT (n=15). Kumpulan MIA dan ACLT dibahagi kepada minggu ke-4 (n=5), ke-8 (n=5) dan ke-12 (n=5). Sendi lutut kanan arnab daripada setiap kumpulan telah dikumpul pada minggu ke-4, ke-8 dan ke-12 dan dinilai dengan menggunakan tomografi berkomputer mikro (mikro-CT) untuk menganalisis perubahan tulang subkondral. Gambar mikro-CT telah ditafsirkan dengan menggunakan Skyscan CT-Analyser Software bagi mendapat mikroarkitek parameter. Data daripada mikro-CT telah dianalisis secara statistical dengan membuat ANOVA empat hala bagi data BV/TV, BS/TV and Tb.Sp diikuti oleh ujian *post-hoc Tukey* manakala *Kruskal Wallis H test* telah digunakan bagi data Tb.Th. Hasil menunjukkan bahawa pembentukan semula tulang di medial dan lateral condyles adalah berbeza antara satu sama lain. Medial condyle menunjukkan lebih banyak perubahan disebabkan oleh ketidakseimbangan tulang penyerapan semula dan pembentukan proses. Selain itu, kehilangan subkondral bone akan berlaku pada peringkat awal tetapi apabila penyakit berterusan, tulang subkondral sclerotik akan meningkat dan mengeras.

Kata Kunci: osteoarthritis, ligament krusiat hadapan, monosodium iodoacetate, tomografi berkomputer mikro, arnab

EVALUATION OF MICROMORPHOLOGICAL CHANGES OF THE LATERAL AND MEDIAL CONDYLE OF THE FEMUR AND TIBIA IN BOTH SURGICALLY AND CHEMICALLY INDUCED OSTEOARTHRITIC KNEE IN RABBIT MODEL

Yee Xue Rou & [1]Lau Seng Fong

[1]Department of Veterinary Clinical Studies

Faculty of Veterinary Medicine

Universiti Putra Malaysia, 43400 UPM Serdang, Selangor Darul Ehsan, Malaysia

*Correspondence : lausengfong@upm.edu.my

ABSTRACT

Osteoarthritis is caused by inflammation, breakdown, and eventual loss of cartilage in the joints. Diagnosis of early stage of osteoarthritis is still under investigation due to the complicated pathogenesis of the disease. There are limited studies about the differences between the changes in medial and lateral condyle in knee joint during osteoarthritis thus this research was carried out. The objective of this study was to detect and evaluate the micromorphological changes in medial and lateral condyle in osteoarthritic femur and tibia such as bone to tissue volume (BV/TV), bone surface density (BS/TV), bone surface to volume ratio (BS/BV), trabecular thickness (Tb.Th) and trabecular seperation (Tb.Sp) in chemically-induced osteoarthritis and surgically-induced osteoarthritis at different time point (Week 4, 8 and 12). Thirty-

five adult New Zealand white rabbits (n=35) were divided into three groups: Control (n=5), MIA (n=15) and ACLT (n=15). MIA and ACLT induced osteoarthritis were further divided into Week 4 (n=5), Week 8 (n=5) and Week 12 (n=5) groups. Right femur and tibia of each group of rabbit were harvested at different point of time and evaluated with micro-computed tomography (micro-CT) for the changes in the subchondral bone.. Data obtained from micro-CT were analysed statistically by performing factorial ANOVA for BV/TV, BS/TV and Tb.Sp followed by post-hoc Tukey test whereas Kruskal Wallis H test for Tb.Th. Results showed statistical significantly different ($p<0.05$) in BV/TV for medial and lateral condyles of femur and tibia at different point of time however the method of induction showed no statistical significantly different ($p>0.05$) in BV/TV. . The results indicate that the bone remodelling on both medial and lateral condyles were different from each other. Medial condyle showed more changes in subchondral bone due to imbalance bone reabsorption and formation process. Besides, there will be loss of subchondral bone in the early stages of OA but as disease progress there will be increase stiffening of sclerotic subchondral bone.

Keywords: *osteoarthritis, anterior cruciate ligament, monosodium iodoacetate, micro-computed tomography, rabbits, medial condyle, lateral condyle*

Introduction

Osteoarthritis (OA) is a degenerative joint disease usually progress slowly involving all joint tissues which eventually lead to joint disability and pain. Osteoarthritis involves degradation of articular cartilage, restructuring of subarticular bone, osteophyte formation, ligamentous laxity, synovial inflammation and weakening of periarticular muscles (Anna *et al*., 2013).

Osteoarthritis takes up 2.4% of all year lived with disability (YLD) and is the 10th primary contributor to global YLDs with hip and knee osteoarthritis accounts 5% of the global population (OARSI, 2016). Although osteoarthritis is primarily thought to be cause by aging, traumatic sports injuries, obesity, sex, smoking, osteoporosis, sarcopenia, local mechanical risk factor, inflammation, and genetic predisposition (Chen *et al*., 2017 ; Anna *et al*., 2013), its mechanism is still not fully known.

The study of pathogenesis of osteoarthritis commonly used animal models (Chen *et al*., 2017). Animal models are divided into two groups which are the small animal (mouse, rat, rabbit, and guinea pig) and large animal group (dog, goat/sheep, and horse). Small animal mostly used in studying pathogenesis and pathophysiology of disease while large animal mostly used in studying disease process and treatment. Stifle joint is commonly used in small animals while metacarpophalangeal is regularly used in horse because it has the greatest similarity to human knee joint (Kuyinu *et al*., 2016). Rabbits are widely used due to its readily available guidelines for handling, carrying and husbandry. Besides, rabbits are also low cost and easier to handle (Little & Smith, 2008).

Osteoarthritis in animal models can be surgically- induced and chemically-induced. Examples of surgically-induced osteoarthritis are anterior cruciate ligament transection (ACLT), meniscectomy (MNX) and medial meniscal transection (MMT) while chemically-induced osteoarthritis are sodium monoiodoacetate-induced OA (MIA) and carrageenan-induced OA(CAR) (Kuyinu *et al*., 2016). The results of surgically- induced OA are progress quickly while chemically-induced OA avoid possible contamination happens in surgical approach and results progress slowly. The results of surgically-induced OA are highly uniform and progress rapidly but may be too quick to observe the early stages in OA development and early drug treatment while chemically-induced OA avoid any possible contamination during surgical induction and results progress slowly (Cucchiarini *et al*., 2016).

The objectives of this study is to detect and evaluate the micromorphological changes in medial and lateral condyle in osteoarthritic femur joint such as bone to tissue volume (BV/TV), bone surface density (BS/TV), bone surface to volume ratio (BS/BV), trabecular thickness (Tb.Th), trabecular seperation (Tb.Sp), and total porosity (%) in chemically-induced osteoarthritis and surgically-induced osteoarthritis at different time point. The hypothesis were:

Statistical Hypothesis : Chemically- induced osteoarthritis limb will have micromorphological differences when compared to surgically- induced osteoarthritis.

Null Hypothesis : There is no micromorphological differences between chemically-induced osteoarthritis and surgically- induced osteoarthritis.

Alternative Hypothesis: There is micromorphological differences between chemically- induced osteoarthritis and surgically- induced osteoarthritis.

Literature Review

2.1 Stifle Joint

Stifle joint is the largest joint in the hind limb. Stifle joint is a complex condylar synovial joint with separation of its articular surface by intra-articular fibrocartilages (menisci). It consists of three articulations. First is the femoropatellar joint which is found between the patella and distal femur. Next are medial and lateral femorotibial joint which located between medial and lateral condyles of the femur and medial and lateral condyles of the tibia. A single articular capsule enclosed all the articulations (OpenStax.,2013).

Femoropatellar joint consists of suprapatellar pouch, suprapatellar, suprapatellar adipose tissue, patella, medial and lateral proximal recesses, medial and lateral trochlear ridges of the femur and femoral trochlear groove while femorotibial joint consists of cranial cruciate ligament, caudal cruciate ligament, medial and lateral menisci, medial and lateral femoral condyles, long digital extensor tendon and cranial meniscal ligaments (Peters *et al*., 2018). Stifle joint is like human knee joint.

Anterior cruciate ligament and posterior cruciate ligament are two intracapsular ligaments that help to resist knee hyperextension. These ligaments attached inferiorly to the tibia at the intercondylar eminence, the roughened area between the tibial condyles. The two ligaments crossing each other forming the X-shape and attach to the inner aspect of a femoral condyle (OpenStax., 2013).

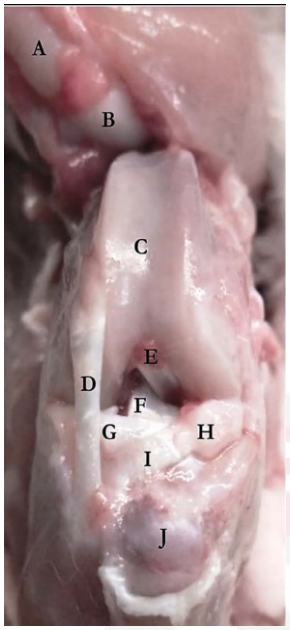

Figure 2.1 Cranial view of a right rabbit stifle in flexion.
The tendon of insertion of the quadriceps, containing the patella (A) and suprapatellar (B), has been transected at its insertion on the tibial plateau (J) and reflected proximally. The medial and lateral trochlear grooves of the femur are readily identified on either side of the patellar groove of the femur (C). The origin of the long digital extensor tendon (D) is present originating from the extensor fossa on the lateral aspect of the femur. The caudal (E)
and cranial (F) cruciate ligaments are apparent and the cranial ligament of the medial meniscus (I) is seen cranial to both the medial (H) and lateral (G) horn of the meniscus. The cranial ligament of the lateral meniscus is not apparent from this view, but extends from the cranial aspect of the meniscal horn medially, to insert on the proximal tibia just distal to the craniomedial aspect of the medial meniscus. The picture is courtesy of Arthroscopic approach and anatomy of the stifle joint in the rabbit. Veterinary Surgery, 47(1), 130-135

Figure 2.2 Anatomy of Knee Joint Labeled Knee Joint Anatomy Labeled

(Pictures courtesy of Senin, 2019)

2.1.2 Articular cartilage

Normal adult articular cartilage is made up of extracellular matrix which consists of water, collagen fibrils, proteoglycans, fibronectin, elastin, other noncollagenous structural proteins, a very small component of calcium salt and few chondrocytes (Goldring *et.al.,* 2010; Danila, 2014). It is made up of hyaline cartilage and covers the articulating bony surfaces. The functions of articular cartilage are lower the friction during joint movement, absorbs the biomechanical forces, and stabilizes the joint. Cartilage is avascular so it depends on synovial fluid and subchondral bone to nourish the surface of articular cartilage and base of articular cartilage respectively (Moore, n.d.). It also depends on anaerobic metabolism (Buckwalter, 1997; Man & Mologhianu, 2014).

In an adult, chondrocyte is important in development, maintenance and repair of the extracellular matrix by mediates synthetize matrix components and the proteolytic enzymes for their breakdown (Wise, 2010; Man & Mologhianu, 2014). Collagen turnover rate is relatively slow, whereas proteoglycan turnover rate is rapid (Mow *et.al*., 2005). Polypeptide growth factors and cytokines, structural and physical stimuli and components of matrix itself affect chondrocytes (Wise C., 2010).

Normal articular cartilage structure and function are maintained by joint motion and load. Degradation of cartilage caused by inactivity of the joint. Dramatic changes in the cartilage metabolism which is physiological imbalance of degradation and synthesis by chondrocytes leads to development of disease such as osteoarthritis (Man, G. S., & Mologhianu, G., 2014).

2.1.3 Subchondral Bone

Subchondral bone divided into two parts which is known as subchondral bone plate and subchondral trabecular bone (Goldring, 2010). Subchondral bone plate located beneath the articular cartilage and it possesses an irregular surface where articular cartilage attached to. Zone of calcified cartilage divide the articular cartilage and subchondral bone. Trabecular subchondral bone is located under the thin subchondral bone plate. It contains fatty bone marrow and trabecular bone (Martel-Pelletier *et.al*., 2007). Subchondral bone plate has many pores which invaded by channels that provide a direct link between articular cartilage and subchondral trabecular bone. Many arterial terminates at the subchondral bone plate (Martel-Pelletier *et.al.*, 2007). Numerous venous vessels and nerves also penetrate these channels and branches into cartilage (Mandry *et.al*., 2010; Holmdahl *&* Ingelmark, 1950). Subchondral bone end plate's thickness and blood supply depends on age, body weight, location, function and genetics. Central of weight bearing area is normally much thicker. Subchondral bone absorbs shock better than articular cartilage although it is a harder tissue as compared to articular cartilage. Subchondral trabecular bone functions to absorb shock caused by excessive loads and provide nutrient and metabolism to articular cartilage as it contains blood vessels, sensory nerves and bone marrow (Li *et al*, 2013; Martel-Pelletier *et.al.*, 2007).

2.2 Osteoarthritis

2.2.1 Definition of osteoarthritis

According to Li *et al*., 2013, osteoarthritis defined as disability in aging population commonly leads to pain as it is slow progressive degenerative joint disorder characterized by cartilage degradation, thickening in subchondral bone, osteophytes formation, muscle weakness and different degree of inflammation in synovium tissue and tendon, degeneration of ligaments and menisci of the knee and hypertrophy of the joint capsule. Osteoarthritis is a process of wear and tear and also an abnormal remodeling of joint tissues caused by the inflammatory mediators (Loeser *et al*., 2012). Osteoarthritis is being described as a multifactorial disease related to age, sex, previous joint injury, obesity, genetic predisposition and mechanical factors, including malalignment and abnormal joint shape (Li *et al.*, 2013). OA are divided into primary (idiopathic) and secondary OA based on disease etiology (Altman RD, 1991; Kuyinu *et al.*, 2016). Primary OA is a naturally occurring degeneration of the joint whereas secondary OA is related to causes and / or risk factors contributing to development of OA in the joint. Primary OA can be divided into localized OA where only one joint affected or generalized OA where three or more joints are affected. Risk factors leads to development of secondary OA are trauma, congenital diseases and other diseases or disorder of metabolism of the bone (Altman R *et al.*, 1986; Kuyinu *et al.*, 2016).

Osteoarthritis only detected after onset of pain during late stage therefore there is limited ability to detect osteoarthritis in early stage before onset of pain (Liu *et al.,* 2016). Besides, molecular mechanism involved in OA initiation is not well known.

These result in no present interventions to repair degenerated cartilage or reduce speed of disease progression (Chen *et al.,* 2017).

2.2.2 Biomechanical weight bearing in rabbit and human

Rabbit hindlimb has been extensively used as an animal model in various types of orthopaedic research despite unclear biomechanics of normal rabbit knee joint (Gushue *et al*., 2005). Rabbit knee is anatomically similar to human knee (Athanasiou *et al*., 1991) except for a smaller patella relative to other structures (Gregory *et al*., 2012). However, rabbit knee has marked difference with higher degree of flexion from human. Therefore, gait and joint biomechanics are significantly differences from human (Laverty *et al*., 2010). Rabbit bears weight more on the lateral compartment of the femoratibial joint rather than medial compartment (Athanasiou *et al*., 1991; Gushue *et al*., 2005) which is different from human where medial compartment bears more weight (Johnson *et al*., 1980; Gushue *et al*., 2005). Thus, medial compartment weight bearing has correlated with the presence of medial compartmental OA (Gushue *et al*., 2005). Rabbit has four legs with weight distributed to four legs while human has two legs where the weight distributed to two legs. Magnitude of the ground reaction forces decreased as the body weight unloading increased. Rabbit's forelimb vertical ground reaction force magnitudes were higher than hindlimb during hopping and both hindlimbs were evenly and simultaneously loaded (Gushue *et al*., 2005). Thus, hindlimb bears more weight than forelimb in rabbit. There is a large variation in kinematic of hindlimb position results in two landing patterns that can be distinguished by variations in the magnitude of the external knee abduction moment. The two landing patterns are

valgus and neutral landing pattern. Valgus landing pattern has significant greater lateral tibiofemoral joint contact forces during the stance phase than neutral landing pattern (Gushue *et al*., 2005).

Generally, load-bearing of joints are supported by subchondral bone and cartilage which are the dynamic stress bearing structures (Pan *et al.,* 2009). Subchondral bone helps articular cartilage to distribute mechanical loads by gradual transition of stress and strain across the joint surfaces. Therefore, secondary cartilage damage and degradation of overlying cartilage occurred when subchondral bone becomes stiffened and less flexible due to increase transmission of loads to the cartilage (Goldring M & Goldring S, 2010).

2.2.3 Osteoarthritis changes in articular cartilage and subchondral bone in medial and lateral condyles in rabbit.

During early stage of osteoarthritis of rabbit caused by ACTL, subchondral bone shows significant thinning and trabecular bone volume and thickness decreased on medial femoral condyle only due to ACTL which reduced joint loading at the medial compartment. However, cartilage structure had more severe changes in the lateral compartment without any alterations in the underlying bone (Florea *et al*., 2015).

During late stage of OA, subchondral bone plate shows thickening (Shimizu *et al.,* 1993) and an increase in the trabecular bone volume fraction in both medial and lateral condyles (Matsui *et al.,* 1997).

ACTL leads to joint instability by abnormal anterior-posterior and rotational motions (Nigg & Herzog, 2007). These would results in modified contact pressures, stress distributions and diminished muscle function (Herzog *et al*., 1998). Unloaded joint

compartment leads to imbalance bone reabsorption and formation process will have adaptive bone remodeling process, decreased trabecular bone volume fraction and trabecular thickness (Florea *et al*., 2015).

Second, early subchondral bone remodeling is associated with the activation of osteoclast formation by inflammatory response (Yoneda, 1993) or by increased blood flow in the subchondral bone (Judex *et al*., 1997). Both processes increase the subchondral and trabecular bone loss in the medial part of the bone.

Thirdly, lateral compartment of the femoral condyle has no changes due to distribution of forces from cartilage into bone and normal bone remodeling in lateral side. Besides, lateral side has faster adaptive process to recover from the possible initial loss of mass (Florea *et al*., 2015).

Moreover, loss of prostaglandins, disorganization of the collagen fibrils, increased collagen content and changes in the equilibrium modulus of cartilage can be identified. However, more severe changes in articular cartilage occurred in lateral compartment without involvement of subchondral bone changes. Accelerated bone resorption in medial femoral condyles causes reduced in subchondral bone thickness, bone volume fraction and trabecular thickness. Thinning of subchondral bone caused by OA whereas losing of trabecular bone is a result of altered joint loading due to ACTL. Thinning of subchondral bone plate leads to increase in cartilage damage (Florea *et al*., 2015).

MIA injection inhibits glyceraldehydes-3-phosphate dehydrogenase, a key enzyme in glycolysis cause decrease in intracellular ATP which leads to progressive cellular apoptosis, a decrease in glycosaminoglycans and sclerosis of the subchondral bone in the bearing area of the cartilage as observed in human (Mohamed *et al*., 2020).

The articular cartilage acts as a cushion or a shock absorber when sheer stress is placed on the knee (Radin & Rose, 1986). When repeated mechanical load is placed on the joint, microdamage to the underlying subchondral bone enhances bone turnover causing sclerosis and stiffening (Muraoka *et al.*, 2007). As the articular cartilage lies on top of the subchondral bone, the substantial gradient in stiffening of the underlying layer of subchondral bone caused an upward shear stresses in the cartilage, resulting in cartilage fibrillation. This then leads to cartilage degeneration which fuels OA progression.

2.2.4 Pathogenesis of Osteoarthritis in subchondral bone

Subchondral bone changes remains a controversy whether it happens prior to articular cartilage changes or it happens in the disease development due to adaptation processes after changes in the biomechanical properties of the articular cartilage (Li *et al.,* 2013; Man & Mologhianu; 2014). But, both processes are interrelated as proposed by the associated increase in the levels of cartilage oligomeric matric protein (COMP) and bone sialoprotein (BSP) in early stage of OA (Aigner & Schmitz; 2011; Man & Mologhianu; 2014). Subchondral bone properties are mediated by the process of remodeling (reabsorption and formation of new bone on previously reabsorbed surface) and bone modeling (architecture and bone volume changes via direct apposition to existing bone surface) (Goldring MB & Goldring SR; 2010). Alteration of all these mechanisms during osteoarthritis cause structural changes in subchondral bone. Sclerotic changes, bone marrow lesions development and bone cyst occurred in subchondral compartment during OA (Man & Mologhianu,

2014). Subchondral bone sclerosis normally happens in the later stage of OA (Intema *et al*., 2010) and is an undeniable sign of OA (Wang *et al*., 2010).

In early stages of OA, elevated bone remodeling and subchondral bone loss occurred in human whereas subchondral bone microstructural damage by increased remodeling followed by osteoporosis and subchondral bone loss observed in rabbit model (Li *et al.*, 2013) In age related OA, aging of the musculoskeletal system increases the susceptibility to OA but alone does not cause the development of OA. During aging process, the ability of cells and tissues in the body to maintain homeostasis loss, particularly when put under stress (Ferrucci *et al*., 2002). Thus excessive or abnormal mechanical stresses cause development of OA faster when aged (Shane & Loeser, 2010). Cartilage damage strongly related to thinning and increased porosity of the subchondral bone plate and then followed by thickening of the cortical plate as OA progress (Batiste *et al*., 2004). Increased trabecular separation, decreased bone volume fraction and trabecular thickness were seen in subchondral trabecular bone during early OA (Batiste *et al*., 2004; Wang *et al*., 2010; Li *et a*l., 2013). Elevation of cross-linked N-telopeptide of type I collagen (NTx) and Ctelopeptide (CTx) during osteoarthritis indicates bone reabsorption with progressive loss of trabecular bone (Man & Mologhianu; 2014).

Characteristics of later stages are elevated apparent density, increased bone volume, thickening of subchondral bone plate, increased trabecular thickness, decrease of trabecular separation and bone marrow spacing, and transformation of trabeculae from rod-like into plate-like (Ding, 2010). Osteophytes form at the joint margin. Although there is increased bone volume density which is known as ‘sclerotic’ subchondral bone but there is reduced in the mineralization of bone. Type I collagen

synthesis is elevated in subchondral bone but deposited collagen is hypomineralized and low calcium to collagen ratio (Mansell & Bailey, 1998; Li *et al*., 2013). This is followed by increase trabecular number and volume creating apparent stiff structure. Subchondral bone cyst pathogenesis of formation still unclear but there is two hypothesis, 'synovial fluid intrusion' theory or 'bone contusion' theory. In 'synovial fluid intrusion' theory, synovial fluid with growth factors penetrate into bone marrow through total damaged of osteochondral junction to form bone cyst and induce fibrocytic and chondrometaplastic changes (Durr *et al*., 2004; Li *et al*., 2013). In 'bone contusion' theory, abnormal mechanical stress and subsequent microcracks, edema and focal bone resorption induced necrotic lesions in subchondral bone which eventually leads to subchondral bone cyst (Ondrouch, 1963). According to Man & MOloghianu in 2014, subchondral bone cysts initially contain fluid but become ossify as the OA progress.

Bone marrow edema-like lesions of subchondral bone form due to damaged cartilage which leads to inflammatory reaction in synovial fluid and microtraumatic changes associated with altered biomechanics (Garnero *et al*., 2005). Presence of bone marrow lesions indicates increased metabolic activity and persistence cartilage damage (Man & Mologhianu; 2014).

2.3 Osteoarthritis study in animal model

Animal models are divided into two groups which are the small animal (mouse, rat, rabbit, and guinea pig) and large animal group (dog, goat/sheep, and horse). Small animal mostly used in studying pathogenesis and pathophysiology of disease while large animal mostly used in studying disease process and treatment. Small animal

models are used for therapeutic interventions and initial drug screening studies (Teeple *et al*., 2013; Mitchell *et al*., 2013) followed by further testing in large animal models before clinical trials in human (Pelletier *et al*., 2010 ;McCoy, 2015) and approval therapeutic interventions by regulatory authorities (McCoy, 2015; Kuyinu *et al*., 2016; Samvelyan *et al.,* 2020). Small animal models required relatively low cost, easy to handle and maintain. Large animal models have joint anatomy similar to human including joint size and articular cartilage thickness (Gregory *et al.*, 2012). However, large animal models are more costly, difficult to handle, longer time to age, slower OA progression and ethical consideration (Samvelyan *et al.,* 2020). Stifle joint is commonly used in small animals while metacarpophalangeal is regularly used in horse because it has the greatest similarity to human knee joint (Kuyinu *et al*., 2016). Rabbits are widely used due to its readily available guidelines for handling, carrying and husbandry. Besides, rabbits are also low cost and easier to handle (Little & Smith, 2008).

Advantages and Disadvantages of Species Used in Models of OA

Species	Advantages	Disadvantages
Mouse	Tractable Easy Management Low cost Speed of disease onset is rapid Genetic modifications possible Full genome available Microarray available	Size – limits tissue discrimination and availability Known molecular differences e.g. MMP-1 Limited synovial fluid harvest possible Ratio of cell volume to matrix in

	Low amounts of drug required	cartilage high No regional pathology possible Limited clinical outcomes (MRI, pain etc) Surgical induction more difficult
Rat	As for mouse plus Pain models available	As mouse although surgery is easier
Guinea pig	Tractable Easy Management Spontaneous disease	Size for regional analysis Not available in all countries Lack of full genome
Rabbit	Easy to dose Readily available in most countries Surgically suitable Genetically pure	Prevalent disease Articular cartilage degrades more easily and repairs readily (unlike human) Lack of complete genome
Cat	Size (tissue/ Fluid collection) Regional tissue analysis possible Full genome available Intraarticular therapy possible	Emotional attachment and ethically controversial in many countries ± tractable Management difficult/costly Genetic variability No microarrays available
Dog	Size (tissue/ Fluid collection)	Emotional attachment and

	Tractable and trainable Regional tissue analysis possible Intraarticular therapy convenient Clinical outcome measures well published Full genome available (beagle) Microarray available	ethically controversial in many countries Management difficult/costly Genetic variability Lack of complete genome for other than beagle
Goat	Size (tissue/ Fluid collection) Regional tissue analysis possible Cartilage thickness closer to human's	Cost Lack of complete genome No microarrays available Not monogastric (oral therapy) Housing/management difficult
Sheep	Size (tissue/ Fluid collection/approximates human) Regional tissue analysis possible Housing and availability (country dependent) Control of strain genetics Clinical outcome measures well published Intraarticular therapy convenient	Lack of complete genome No microarrays available (could use bovine) Not monogastric (oral therapy)
Primates	Closest genetically to humans Size (tissue/ Fluid collection)	Full genome not available for some

	Regional tissue analysis possible Genome available for some species Rhesus monkey array available Intraarticular therapy possible	Housing and management difficult Cost Emotional attachment and ethically controversial in many countries
Horse	Size (tissue/ Fluid collection) Regional tissue analysis possible Clinical outcome measures well published Cartilage thickness closer to human's Intraarticular therapy convenient Genome and microarray available	Cost Management, housing (size) Drug amounts required for systemic therapy may be prohibitive Specialised anaesthesia/surgical facilities required

Table 2.1 Animal models with its respective advantages and disadvantages (Little & Smith, 2008).

2.4 Osteoarthritis induction method

Osteoarthritis models can be classified into spontaneous and induced models. Primary osteoarthritis consists of spontaneous, naturally occurring models and genetically modified models whereas secondary osteoarthritis consists of post-traumatic OA which is subdivided into surgically induced and chemically induced OA.

The most common models in surgically induced OA are anterior cruciate ligament (ACLT), menisectomy (partial or total), medial meniscal tear and ovariectomy. Aseptic techniques is important in surgically induced OA. Surgically induced OA induces rapid and severe changes in articular cartilage and subchondral bone which is excellent choice for short-term studies (Kuyinu *et al*., 2016). It also mimic molecular pathology and histopathology observed in human (Little & Smith, 2008). However, the rapid progression of OA makes it difficult to follow early stage of OA development and results of early drug treatment.

Anterior cruciate ligament transection (ACLT) is the earliest well known and most frequently used surgical method to induce OA for research purpose (Kuyinu *et al*., 2016; Samvelyan *et al*., 2020). ACLT causes ACL injury that leads to mechanical instability in the joint. This mimic the pathological changes observed in human with post-traumatic OA (PTOA) (Florea *et al*., 2015; Kuyinu *et al.*, 2016; Samvelyan *et al.,* 2020). ACLT induced OA imitates molecular changes in the cartilage, synovial inflammation and subchondral bone sclerosis in human OA (Kim *et al.*, 2018). ACLT is used to observe structural, compositional and mechanical changes occur in cartilage with different animal models (Florea *et al.*, 2015). Anterior drawer test is done to indicate the success of ACLT (Kuyinu *et al.*, 2016). However, ACLT models will affect gait, initial oxygen tension and content of synovial fluid as it require the opening of the joint cavity (Liu *et al*., 2016). As early as 4 weeks post ACLT, development of disease such as fissures and erosion of cartilage can occur. Cartilage lesions usually observed in femoral condyles and in tibial plateau and lesions are focal in each compartment.

Chemically induced OA is easy to induce and reproduce by injecting toxic or inflammatory compound directly into the joint. Examples of drugs are sodium monoiodoacetate, papain, quinolone and collagenase (Kuyinu *et al*., 2016). Various stages of disease development can be achieved by administration of different dosages and intervals of compounds. This is an excellent model to study OA pain-related behaviours and effects of drugs mainly on pain killer and anti-inflammatory (Kuyinu *et al*., 2016; Samvelyan *et al*., 2020). The advantages are to prevent any possible infections that can occur during surgical method (Kuyinu *et al*., 2016). However, chemically induced OA causes rapid, widespread of cell death and joint changes different from human primary or secondary OA pathophysiology (Samvelyan *et al.,* 2020).

Sodium monoiodiacetate (MIA) is commonly used to study OA (Guingamp *et al*., 1997; Kuyinu *et al.*, 2016) and it induces a joint pathology that mimicking human degenerative OA in terms of the histological and pain-related behaviour (Bove *et al.,* 2003; Moilanen *et al*., 2015). However, MIA induced OA does not have disease process that fully mimic OA process (Little & Smith, 2008). MIA is a metabolic inhibitor of glyceraldehyde-3-phosphate dehydrogenase (GAPDH) in Krebs cycle which inhibits the activity of aerobic glycolysis pathway in chondrocytes leading to chondrocytes death. Formation of osteophytes and degradation of articular cartilage followed after chondrocytes dead (Marker & Pomonis, 2012; Kuyinu *et al*., 2016). This results in rapid inflammation that lasts for 7 days, chronic pain, hyperalgesia and allodynia (Fernihough *et al*.,2004; Kuyinu *et al*., 2016; Samvelyan *et al*., 2020).

2.5 Micro-computed tomography

Micro-CT is x-ray imaging in 3D on a small scale with massively increased resolution and is good for assessing bone morphology and microarchitecture in small animal models (Bakar *et al.*,2019). Micro-CT imaged very fine scale down to 1µm or smaller, internal structure of intact bones without destruction or cutting it into pieces. Micro- CT is commonly used in research to study the bone architecture and density to identify characteristics of osteoporosis and osteoarthritis in appropriate animal models (Holdsworth & Thornton, 2002). Micro-CT allows user to easily measure bone density and differentiate signal contrast between bone and soft tissue. The 3D architecture of the trabecular bone observed can be reformatted into frontal, sagittal and transverse planes for investigation of bone density and architecture (David & Michael, 2002).

2.5.1 Bone parameters

Bone parameters measured in this study are percent bone volume (BV/TV), bone surface density (BS/TV), trabecular thickness (Tb.Th) and trabecular separation (Tb.Sp).

a) Percent Bone Volume, BV/TV (%)

BV/TV is ratio of the segmented bone volume to the total volume of the region of interest. In the other words, BV/TV is the fraction of a given volume of interest (TV) that is occupied by mineralized bone (BV). Unit of BV/TV is percent (%). BV/TV can be obtained directly from 2D images. Two important components of BV/TV are bone volume (BV) and total volume of interest (TV) (Parfitt *et al.*, 1987; Bouxsein *et. al.,*2010) which can be obtained either from a simple voxel-counting method or a

more advanced volume-rendering method, also known as volumetric marching cubes (VOMACs). VOMACs are more accurate for very complex or small structures (Muller & Ruegsegger, 1995; Bouxsein *et. al.,*2010). BV/TV is important to identify relative changes of the bone volume density.

$$Percent\ Bone\ Volume = \frac{Bone\ Volume\ (BV)}{Volume\ of\ Interest\ (VOI)}$$

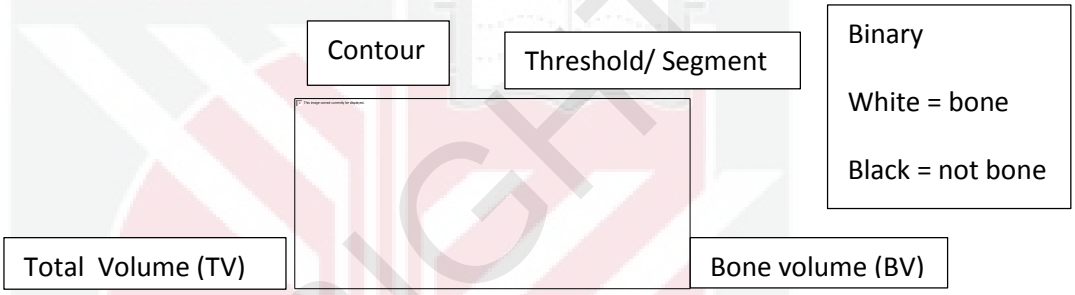

Figure 2.3 Illustration of BS and TV

Source: WU Musculoskeletal Research Center Musculoskeletal Structure & Strength Core, 2018

b) Bone Surface Density, BS/TV (mm^2/mm^3)

BS/TV is ratio of the segmented bone surface to the segmented bone volume. BS/TV can be identified directly from 2D images. Bone surface (BS) is conventionally computed by triangulation of the object surface using a marching-cubes algorithm (Lorensen & Cline, 1987; Bouxsein *et. al.,*2010). BS/TV can be derived easily by dividing bone surface to the total volume and it is an independent measure.

$$Bone\ Surface\ Density = \frac{Perimeter\ (\mu m)}{Tissue\ Area\ (\mu m2)} \times 1000$$

c) Trabecular Thickness, Tb.Th (mm)

Tb.Th is mean thickness of trabeculae, assessed using direct 3D methods. It is measure using the sphere-fitting method where for thickness measurement the spheres are fitted to the structure and identified the diameter of the largest possible sphere that can be fitted through each voxel. Average thickness of the structure can be obtained when the sphere encloses point (but the point is not necessarily the centre of the spheres) and the sphere is entirely bounded within the solid surfaces (Bouxsein *et. al.,*2010). The average diameter of the spheres represents the object thickness.

Figure 2.4 Schematic representation of algorithm used for direct 3D method for calculation of trabecular thickness by fitting the spheres insides the structure.

d) Trabecular Separation, Tb.Sp (mm)

Tb.Sp is mean distance between trabeculae, assessed using direct 3D methods. . It is measure using the sphere-fitting method where for

thickness measurement the spheres are fitted to the background (marrow space) and identified the diameter of the largest possible sphere that can be fitted through each voxel. Average separation of the marrow space can be obtained when the sphere encloses point (but the point is not necessarily the centre of the spheres) and the sphere is entirely bounded within the solid surfaces. The average diameter of the spheres represents the trabecular separation. It can be used to calculate trabecular number (Tb.N).

$$Trabecular\ number = \frac{1}{Trabecular\ Separation\ (mm)}$$

Figure 2.5 Schematic representation of algorithm used for direct 3D method for calculation of trabecular separation by fitting the spheres insides the background.

Method

3.1 Animal Model and housing

Male New Zealand White rabbits (n=35, age 7 months, weight 1.8kg-2.3kg) were used in this study. Seven months old rabbits are chosen because bone physes close and mature enough as models for early osteoarthritis (Madry *et al*., 2012). They were housed individually in stainless-steel cage and fed with commercial rabbit pellets twice daily with fresh water given *ad libitum*. They were placed in Animal Research Facility, Faculty of Veterinary Medicine, Universiti Putra Malaysia. The rabbits were given one week to acclimatize before induction of OA. This study was approved by Universiti Putra Malaysia Animal Care and Use Committee (UPM/IACUC/AUP-R090/2016).

3.1.2 Preparation of animal model of osteoarthritis

Five rabbits out of thirty-five rabbits were randomly selected as the control group. The remaining thirty rabbits are divided into surgically induced OA and chemically induced OA which are anterior cruciate ligament transection (ACLT) and monosodium iodoacetate (MIA) respectively. Each induction method with fifteen rabbits are further divided into different point of time which are week 4 (n=5), week 8 (n=5) and week 12 (n=5).

For ACLT group, Zoletil® (VIrbac, Australia) at 3mg/kg via intramuscular route was used to do general anaesthesia before ACLT. Anterior cruciate ligament located on the right stifle joint was transected. The surgery was maintained by using gas isoflurane.

For MIA group, monosodium iodoacetate (MIA) (Sigma-Aldrich, USA) was diluted using saline to a concentration of 25mg/ml. MIA was injected intra-articularly into the right tibiofemoral joint at 5mg pre joint per rabbit on day one and 7.5mg per joint per rabbit into day four. The tibiofemoral joint has some similarity with human knee thus it was chosen as a site of induction (Laverty et al., 2010). Besides, the volume of synovial fluid collected would be higher in comparison to the other joints. Rabbits were under general anaesthesia using Zoletil® (Virbac, Australia) at 1.5mg/kg via intramuscular route during the induction procedure.

3.1.3 Sample Preparation

Rabbits from each experimental and control group where euthanized using 200mg/kg pentobarbital sodium at week 4, week 8 and week 12. The knee joints were harvested at 4, 8 and 12 weeks for both MIA and ACLT groups. The knee joints were fixed under 10% buffered formalin (Sigma-Aldrich, USA) immediately after harvested. In order to preserve the cartilage surface, muscles and tissues surrounding the femur and tibia were carefully removed. The proximal tibia and distal femur were soaked in 10% buffered formalin until it is observed under micro-CT scanning.

3.2 Micro-computed tomography evaluation

Skyscan 1076 micro-CT scanner (Skyscan, Belgium) scanned the right stifle joint of Control, Week 4, Week 8 and Week 12 for both ACLT and MIA groups and focusing on the proximal tibia and distal femur portions. The scanning parameters were 70kV and 110μA, with a pixel size of 18μm. Settings for the X-ray projections were set at 0.9degrees angular step with a scanning angular range of 360 degrees.

Skyscan NRecon software (Skyscan, Belgium) were used to reconstruct the image slices.

Two dimentional (2D) images were evaluated qualitatively in both dorsal and sagittal planes for morphological alteration that occurred in the different stages of early OA by using DataViewer software (Skyscan, Belgium).

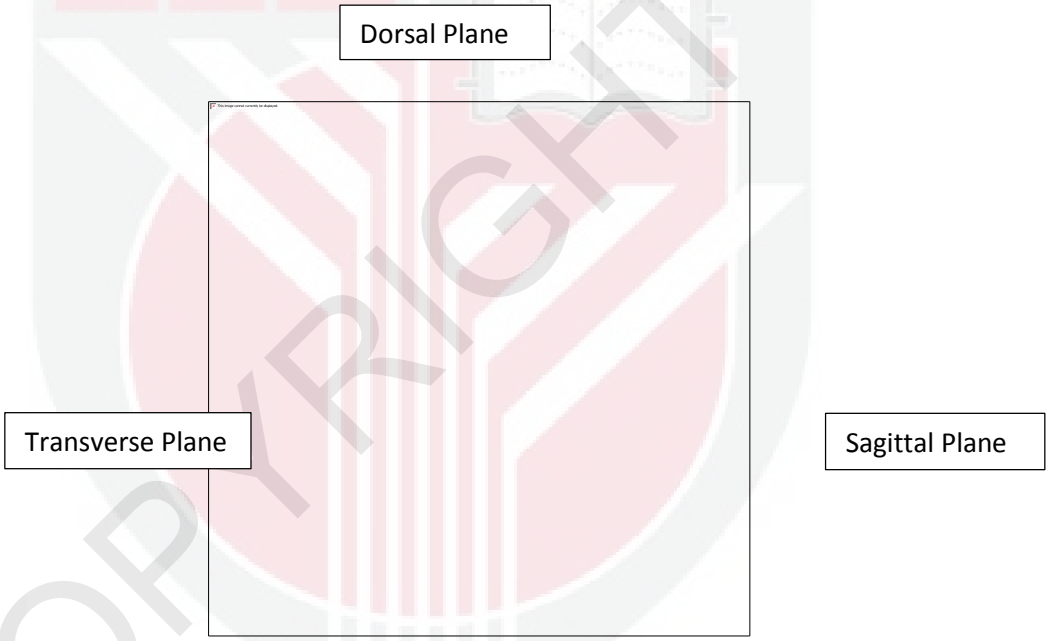

Figure 3.1 2D images from DataViewer software (Skyscan, Belgium)

Micro-CT images were interpreted quantitatively by using Skyscan CT-Analyser Software (Skyscan, Luxemboury, Belgium). Around 2mm of the subchondral bones were selected from each data. The transverse planes of femur or tibia subchondral bone are divided into medial and lateral compartment for analysis. Volume of interest (VOI), consisting of a stack of regions of interest (ROI) was selected from the distal femoral and proximal tibia subchondral bone at the epiphyseal with a

semiautomatic contouring method. The subchondral bone micro-architecture parameters including the ratio of bone volume over tissue volume (BV/TV;%), bone surface density (BS/TV; mm^2/mm^3), trabecular thickness (Tb.Th; mm) and trabecular separation (Tb.Sp; mm) were analysed.

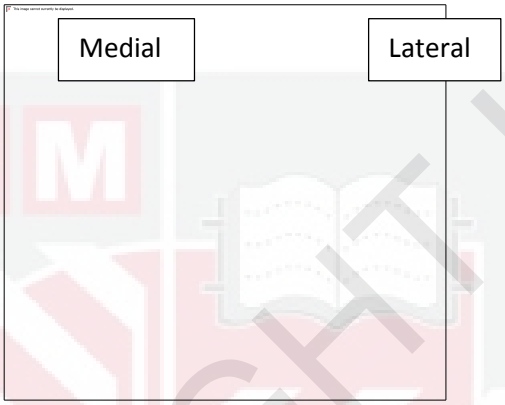

Figure 3.2 Separation of 2D images of femur into medial and lateral compartment.

3.3 Statistical Analysis

Statistical analysis was done to identify the statistical significance differences. The test done was 4-way ANOVA and Kruskal-Wallis H test with Tukey and LSD's Post Hoc test for normally distributed data and not normally distributed data respectively. Percent Bone Volume (BV/TV), Bone Surface Density (BS/TV) and trabecular separation (Tb.Sp) which are normally distributed according to Shapiro-Wilk test are analysed using 3-way ANOVA while trabecular thickness (Tb.Th) which is not normally distributed according to Shapiro-Wilk test is analysed using Kruskal-Wallis H test.

IBM SPSS statistic version 25 software (USA) were used to do statistical analysis. Differences between the groups will be consider significant if p value is <0.05. The

data used for analysis were divided into four dependent variables and four independent variables. Interaction between the four independent variables were took into consideration. Each independent variables were analysed separately (BV/TV, BS/TV, Tb.Th, Tb.Sp).

4.0 Results

4.1 Micro-computed tomographic findings

Quantitative bone micro-architecture assessment

Parameters of the bone micro-architecture that were obtained from the Skyscan CT-Analyser Software include percent bone volume (BV/TV), bone surface density (BS/TV), trabecular thickness (Tb.Th) and trabecular separation (Tb.Sp). The values extracted from each sample for MIA and ACLT induction of osteoarthritis in both femur and tibia were tabulated in the tables below. Table 3.1 and 3.2 show the parameters of microarchitecture of subchondral bone of the right stifle joint of femur and tibia respectively from chemically induced osteoarthritis rabbit model. Table 3.3 and 3.4 show the parameters of microarchitecture of subchondral bone of the right stifle joint of femur and tibia respectively from surgically induced osteoarthritis rabbit model. All microarchitecture parameters in subchondral bone of chemically induced OA of femur decrease in week 4. Most medial condyle parameters increase in week 8 however lateral condyle parameters still continue to decrease in week 8 and only started to increase in week 12.

Subchondral Bone of Chemically Induced OA of Femur

	BV/TV (%)		BS/TV (mm^2/mm^3)		Tb.Th (mm)		Tb.Sp (mm)	
	Medial	Lateral	Medial	Lateral	Medial	Lateral	Medial	Lateral
Control	38.24± 1.57	39.07± 2.40	7.05± 0.20	6.59± 0.53	0.17± 0.02	0.18± 0.02	0.38± 0.03	0.40± 0.04
Week 4	37.35± 4.68	42.38± 2.79	6.75± 0.14	6.86± 0.53	0.17± 0.02	0.18± 0.01	0.38± 0.02	0.36± 0.05
Week 8	39.56± 1.99	40.17± 2.41	6.40± 0.34	6.24± 0.06	0.19± 0.01	0.19± 0.01	0.43± 0.04	0.42± 0.01
Week 12	37.48± 3.35	37.48± 3.35	6.17± 0.17	6.45± 0.18	0.19± 0.01	0.17± 0.00	0.42± 0.03	0.42± 0.03

Table 3.1 Microarchitecture parameters of the subchondral bone of the right stifle joints of femur obtained from chemically-induced OA in rabbit model.

Most microarchitecture parameters in subchondral bone of chemically induced OA of tibia in medial condyle increase while lateral condyle decrease in week 4. Most medial condyle parameters continue to decrease in week 8 however lateral condyle parameters started to increase in week 8.

Subchondral Bone of Chemically Induced OA of Tibia

	BV/TV (%)		BS/TV (mm^2/mm^3)		Tb.Th (mm)		Tb.Sp (mm)	
	Medial	Lateral	Medial	Lateral	Medial	Lateral	Medial	Lateral
Control	34.32± 1.93	30.21± 1.97	4.59± 1.04	4.46± 1.16	0.26± 0.05	0.24± 0.05	0.64± 0.14	0.65± 0.14
Week 4	39.84± 6.27	26.68± 5.40	5.38± 1.23	4.17± 0.87	0.26± 0.07	0.23± 0.04	0.51± 0.13	0.68± 0.11
Week 8	34.61± 3.41	32.24± 1.96	5.31± 0.22	5.31± 0.19	0.22± 0.02	0.20± 0.01	0.61± 0.02	0.58± 0.02
Week 12	34.39± 3.64	28.26± 1.52	5.55± 0.27	5.59± 0.21	0.21± 0.01	0.18± 0.01	0.56± 0.09	0.55± 0.08

Table 3.2 Microarchitecture parameters of the subchondral bone of the right stifle joints of tibia obtained from chemically-induced OA in rabbit model.

BV/TV and BS/TV microarchitecture parameters in subchondral bone of surgically induced OA of tibia in medial condyle decrease while lateral condyle increase in week 4. Both Tb.Th and Tb.Sp in medial and lateral condyle increase in

week 4. BT/TV for medial condyle only increase in week 12 while BS/TV increase in week 8.

Subchondral Bone of Surgically Induced OA of Femur

	BV/TV (%)		BS/TV (mm^2/mm^3)		Tb.Th (mm)		Tb.Sp (mm)	
	Medial	Lateral	Medial	Lateral	Medial	Lateral	Medial	Lateral
Control	38.24± 1.57	39.07± 2.40	7.05± 0.20	6.59± 0.53	0.17± 0.01	0.18± 0.01	0.38± 0.03	0.40± 0.04
Week 4	36.10± 1.52	40.37± 0.25	6.33± 0.36	6.35± 0.75	0.18± 0.01	0.20± 0.03	0.42± 0.04	0.40± 0.06
Week 8	33.84± 2.71	38.11± 1.42	6.64± 0.10	6.96± 0.33	0.17± 0.02	0.17± 0.01	0.41± 0.03	0.37± 0.02
Week 12	42.09± 0.43	40.45± 2.10	7.13± 0.18	7.03± 0.29	0.18± 0.01	0.17± 0.01	0.35± 0.02	0.36± 0.04

Table 3.3 Microarchitecture parameters of the subchondral bone of the right stifle joints of femur obtained from surgically-induced OA in rabbit model.

Microarchitecture parameters for the subchondral bone of surgically induced OA of tibia in medial condyle decrease until week 8 while lateral condyle started to increase in week 4. The parameters for medial condyle increase only in week 12.

Subchondral Bone of Surgically Induced OA of Tibia

	BV/TV (%)		BS/TV (mm^2/mm^3)		Tb.Th (mm)		Tb.Sp (mm)	
	Medial	Lateral	Medial	Lateral	Medial	Lateral	Medial	Lateral
Control	34.32± 1.93	30.21± 1.97	4.59± 1.04	4.46± 1.16	0.26± 0.05	0.24± 0.05	0.64± 0.14	0.65± 0.14
Week 4	34.64± 0.75	32.77± 1.21	5.68± 0.54	5.47± 0.65	0.21± 0.02	0.21± 0.02	0.54± 0.08	0.55± 0.11
Week 8	29.12± 2.38	29.75± 1.48	5.60± 0.49	5.67± 0.27	0.18± 0.01	0.18± 0.02	0.58± 0.03	0.56± 0.04
Week 12	35.24± 1.25	34.14± 1.77	6.11± 0.21	6.03± 0.41	0.19± 0.01	0.19± 0.03	0.51± 0.04	0.47± 0.04

Table 3.4 Microarchitecture parameters of the subchondral bone of the right stifle joints of tibia obtained from surgically -induced OA in rabbit model.

BV/TV in surgically induced OA (ACLT) on tibia increases from control to week 4 then decreases in week 8 and increases again in week 12. Both lateral and medial tibia shows similar trends. Besides, femur BV/TV of surgically induced OA (ACLT) on lateral femur increases from control to week 4 then decreases from week 4 to week 12. Nonetheless, ACLT on medial femur decreases from control to week 8 and increases in week 12.

Chemically induced OA (MIA) on lateral tibia decreases from control to week 4 then increases in week 8 and decreases in week 12 similar to ACLT. MIA on medial shows an increase from control in week 4 and decrease from week 8 to week 12. Moreover, chemically induced OA (MIA) on lateral femur increases from control to week 4 then decreases from week 4 to week 12. MIA on medial shows a decrease from control to week 4 then increase in week 8 and decrease in week 12.

BS/TV in surgically induced OA (ACLT) on lateral tibia increases from control to week 12. Nonetheless, ACLT on medial tibia increases from control to week 4 then decreases in week 8 and increases in week 12. In addition, femur BV/TV of surgically induced OA (ACLT) on femur decreases from control to week 4 then increases until week 12. Both lateral and medial femur shows similar trends.

Chemically induced OA (MIA) on lateral tibia decreases from control to week 4 then increases until week 12. MIA on medial tibia hasan increase from control to week 4 and decrease in week 8 and increases in week 12. Chemically induced OA (MIA) on lateral femur increases from control to week 4 then decreases in week 8 and increases in week 12. MIA on medial femur shows a decrease from control to week 12.

Tb.Th in surgically induced OA (ACLT) on tibia decreases from control to week 8 then increases to week 12. Both lateral and medial femur shows similar trends. Femur Tb.Th of surgically induced OA (ACLT) on lateral femur increases from control to week 4 then decreases until week 8 and remain constant until week 12. Moreover, ACLT on medial femur increases from control to week 4 then decreases in week 8 and increases in week 12.

Chemically induced OA (MIA) of lateral tibia decreases from control until week 12. MIA on medial remains constant from control to week 4 and decrease until week 12. Chemically induced OA (MIA) on lateral femur remains consistent from control to week 4 then increases in week 8 and decreases in week 12. MIA on medial remains constant from control to week 4 then increases to week 8 and remain constant to week 12.

Tb.Sp in surgically induced OA (ACLT) on tibia decreases from control to week 4 then increases in week 8 and decreases in week 12. Both lateral and medial femur shows similar trends. Femur Tb.Sp of surgically induced OA (ACLT) on femur increases from control to week 4 then decreases until week 12. Both lateral and medial femur shows similar trends.

Chemically induced OA (MIA) of lateral tibia increases from control until week 4 and then decreases until week 12. MIA on medial decreases from control to week 4 then increase in week 8 and decrease in week 12. Chemically induced OA (MIA) on lateral femur decreases from control to week 4 and remain the same in week 8 and week 12. MIA on medial decreases from control to week 4 then increases to week 8 and decreases in week 12.

The results presented were distribution of data based on five summary which are minimum, first quartile (Q1), median, third quartile (Q3) and maximum.

Percent Bone Volume, BV/TV (%)

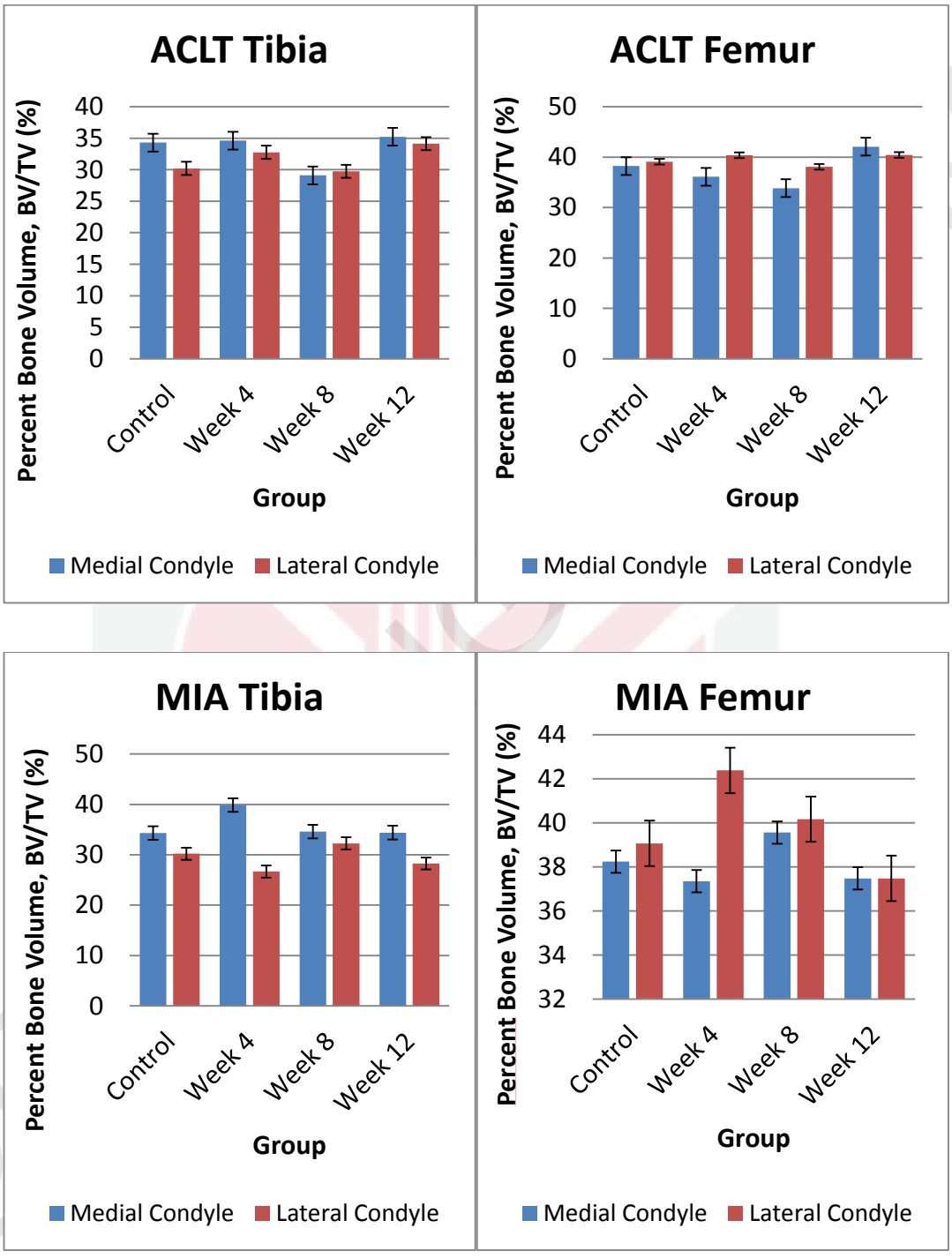

Figure 4.1 Bar Chart of percent bone volume, BV/TV for both medial and lateral of tibia and femur in MIA and ACLT method of induction.

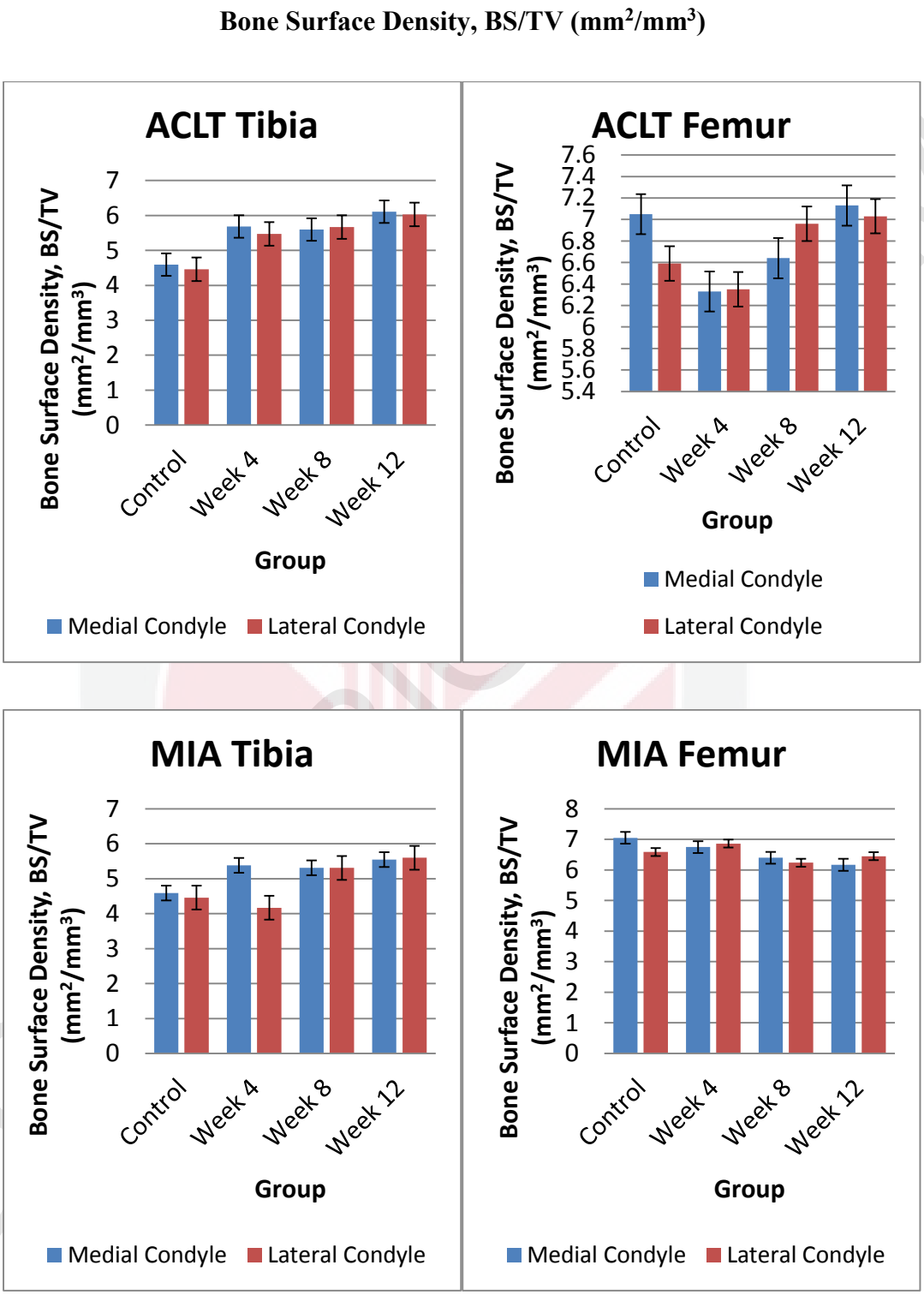

Figure 3.2 Bar chart of bone surface density, BS/TV for both medial and lateral of tibia and femur in MIA and ACLT method of induction.

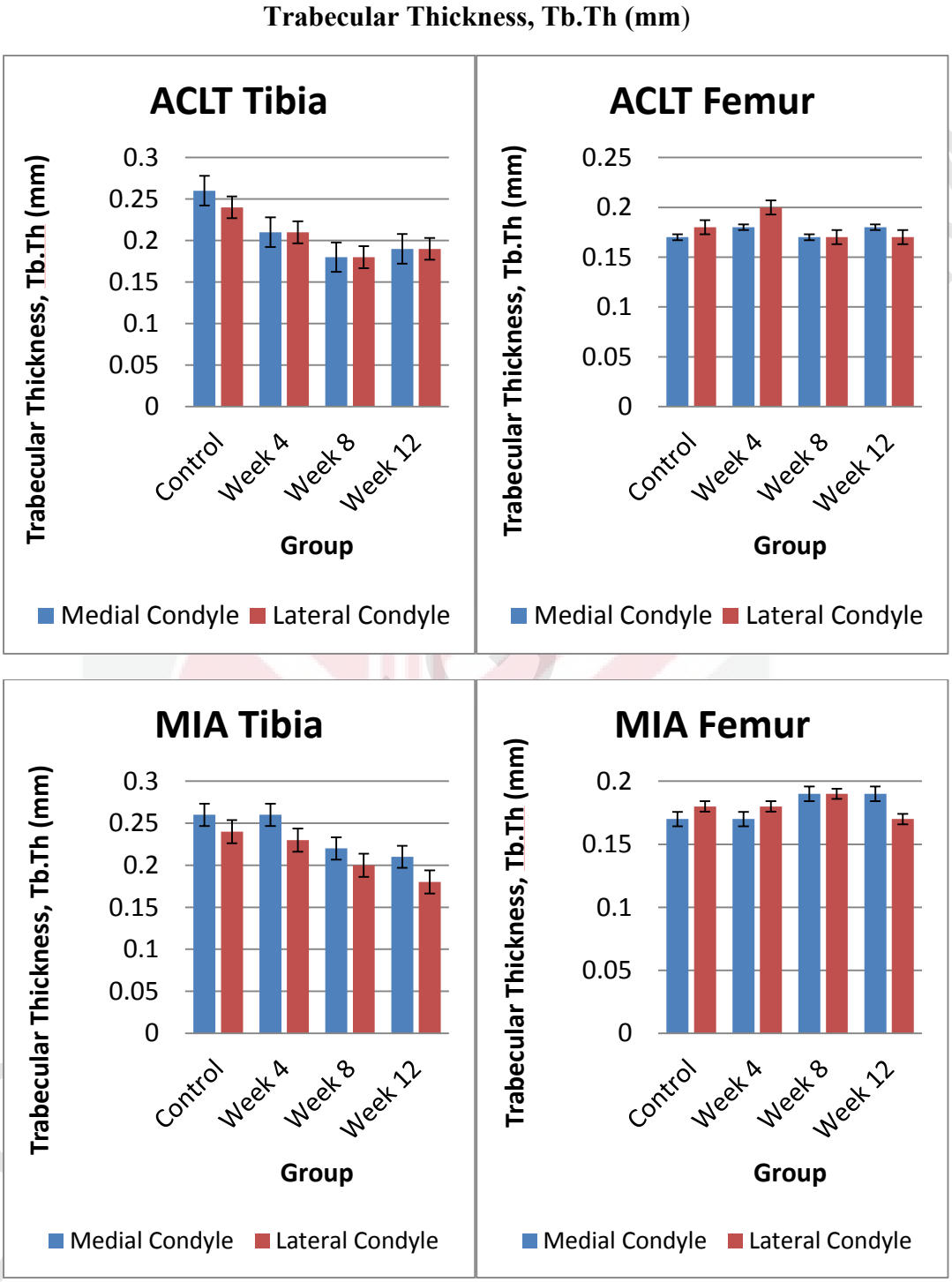

Figure 3.3 Bar chart of trabecular thickness, Tb.Th for both medial and lateral of tibia and femur in MIA and ACLT method of induction.

Trabecular Separation, Tb.Sp (mm)

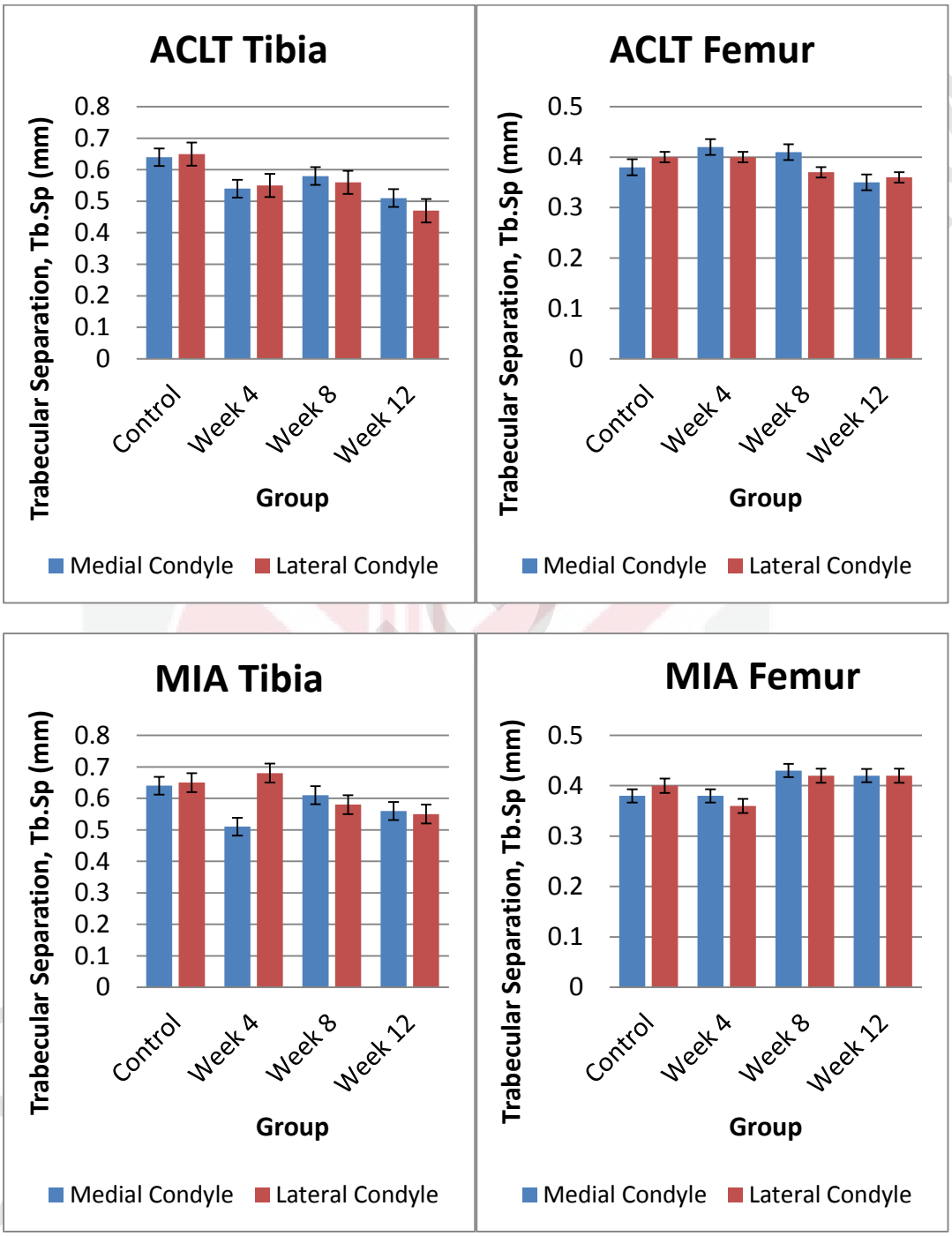

Figure 3.4 Bar chart of trabecular thickness, Tb.Sp for both medial and lateral of tibia and femur in MIA and ACLT method of induction.

BV/TV

According to the univariate test (4-way ANOVA), the main effects for BV/TV due to the parts of bone (p=0.00), time to harvest knee joint (p=0.031) and location on bone (p=0.013) are statistically significant ($p < 0.05$). However, induction method (p=0.399) shows no significant differences ($p < 0.05$).

In first order interactions, four out of six interactions show statistically significant differences as p< 0.05. In second order interactions, two out of four interactions show statistically significant differences as p< 0.05. Third order interaction shows statistically significant as p=0.22.

Sources	Sig. (<0.05)
Parts of bone	.000
Induction method	.399
Time to harvest knee joint	.031
Location (Medial or lateral)	.013
Parts of bone * Induction method	.608
Parts of bone * Time to harvest knee joint	.527
Parts of bone * Location	.000
Induction method * Time to harvest knee joint	.000
Induction method * Location	.001
Time to harvest knee joint * Location	.016
Parts of bone * Induction method * Time to harvest knee joint	.498
Parts of bone * Induction method * Location	.004
Parts of bone * Time to harvest knee joint * Location	.000
Induction method * Time to harvest knee joint * Location	.458
Parts of bone * Induction method * Time to harvest knee joint * Location	.022

Table 3.5. Results of the 4-Way ANOVA Testing for percent bone volume (BV/TV), as a Dependent Variable, and parts of bone, time to harvest knee joint, induction method and location on bone as Combinations of Independent Variables.

Post Hoc Tukey HSD test reveals that there are no significant differences in time to harvest in week 4 , week 8 and week 12 as the significant differences >0.05. However, there is significant differences in time to harvest where p= 0.21 in week 4 and week 8 in LSD test.

Post Hoc Test	Time (i)	Time (j)	Sig.
Tukey HSD	Week 4	Week 8	.053
		Week 12	.683
	Week 8	Week 4	.053
		Week 12	.341
	Week 12	Week 4	.683
		Week 8	.341
LSD	Week 4	Week 8	.021
		Week 12	.408
	Week 8	Week 4	.021
		Week 12	.163
	Week 12	Week 4	.408
		Week 8	.163

Table 3.6. Results of the post hoc for time to harvest knee joint.

BS/TV

According to the univariate test (4-way ANOVA), the main effects for BS/TV due to the parts of bone (p=0.00), time to harvest (p=0.047) and induction method (p=0.006) are statistically significant ($p < 0.05$). However, location (p=0.470) shows no significant differences ($p < 0.05$) and is supported by post hoc Tukey HSD test.

In first order interactions, one out of six interactions show statistically significant differences as p< 0.05 which is interaction between parts of bone and induction method (p=0.037). In second order interactions, one out of four interactions show statistically significant differences as p< 0.05 which is interaction of parts of bone,

induction method and time to harvest knee joint (p=0.027). Third order interaction shows no statistical significant.

Sources	Sig. (<0.05)
Parts of bone	.000
Induction method	.006
Time to harvest knee joint	.047
Location (Medial or lateral)	.470
Parts of bone * Induction method	.037
Parts of bone * Time to harvest knee joint	.236
Parts of bone * Location	.712
Induction method * Time to harvest knee joint	.327
Induction method * Location	.809
Time to harvest knee joint * Location	.390
Parts of bone * Induction method * Time to harvest knee joint	.027
Parts of bone * Induction method * Location	.295
Parts of bone * Time to harvest knee joint * Location	.427
Induction method * Time to harvest knee joint * Location	.491
Parts of bone * Induction method * Time to harvest knee joint * Location	.480

Table 3.7 Results of the 4-Way ANOVA Testing for bone surface density (BS/TV), as a Dependent Variable, and parts of bone, time to harvest knee joint, induction method and location on bone as Combinations of Independent Variables

Post Hoc test indicates that control and chemically-induced OA are significantly differences from surgically-induced OA as p=0.05 and 0.06 respectively. Moreover, time to harvest in week 4 and week 12 shows significant differences as p=0.06.

Post Hoc Test	Induction method (i)	Induction method (j)	Sig.
Tukey HSD	Control	Surgical	.005
		Chemical	.584
	Surgical	Control	.005
		Chemical	.006
	Chemical	Control	.584
		Surgical	.006

Table 3.8 Results of the post hoc for induction method.

Post Hoc Test	Time (i)	Time (j)	Sig.
Tukey HSD	Week 4	Week 8	.299
		Week 12	.006
	Week 8	Week 4	.299
		Week 12	.263
	Week 12	Week 4	.006
		Week 8	.263

Table 3.9. Results of the post hoc for time to harvest knee joint.

Tb.Th

According to the Kruskal Wallis H test, the main effects for Tb.Th due to the parts of bone (p=0.00), are statistically significant ($p < 0.05$). However, induction method (p=0.055), time to harvest (p=0.114) and location (p=0.284) show no significant differences ($p < 0.05$).

Kruskal Wallis H test	Sig. <0.05
Parts of bone	0.000
Induction method	0.055
Time to harvest Knee joint	0.114
Location on bone (medial or lateral)	0.284

Table 3.10 Results of Kruskal Wallis H test for Tb.Th

Tb.Sp

According to the univariate test (4-way ANOVA), the main effects for Tb.Sp due to the parts of bone (p=0.00) and induction method (p=0.037) are statistically significant ($p < 0.05$). However time to harvest the knee joint (p=0.157) and location (p=0.190) show no significant differences ($p < 0.05$) and is supported by post hoc Tukey HSD test.

All interaction of effects shows no significant differences according to ANOVA.

Sources	Sig. (<0.05)
Parts of bone	.000
Induction method	.037
Time to harvest knee joint	.157
Location (Medial or lateral)	.842
Parts of bone * Induction method	.215
Parts of bone * Time to harvest knee joint	.457
Parts of bone * Location	.947
Induction method * Time to harvest knee joint	.269
Induction method * Location	.548
Time to harvest knee joint * Location	.277
Parts of bone * Induction method * Time to harvest knee joint	.369
Parts of bone * Induction method * Location	.304
Parts of bone * Time to harvest knee joint * Location	.171
Induction method * Time to harvest knee joint * Location	.704
Parts of bone * Induction method * Time to harvest knee joint * Location	.418

Table 3.11 Results of the 4-Way ANOVA Testing for trabecular separation (Tb.Sp), as a Dependent Variable, and parts of bone, time to harvest knee joint, induction method and location on bone as Combinations of Independent Variables

Post Hoc test indicates that control and surgically-induced OA are significantly differences from each other as p=0.033. Time to harvest knee joint shows no statistical significant.

Post Hoc Test	Induction method (i)	Induction method (j)	Sig.
Tukey HSD	Control	Surgical	.033
		Chemical	.531
	Surgical	Control	.033
		Chemical	.093
	Chemical	Control	.531
		Surgical	.093

Table 3.12 Results of the post hoc for induction method.

5.0 Discussion

Osteoarthritis started with activation of secondary ossification centre due to subchondral microfractures or inflammation followed by bone resorption by osteoclasts. Then bone formation by osteoblast with bone turn-over rate increased 3-5 times in early OA. Tissue mineralisation attenuated in late phase and lastly, stiffening of subchondral bone (Kuyinu *et al.,* 2016; Donell, 2019). In early stage of OA, increased trabecular separation, decreased bone volume fraction and trabecular thickness were seen in subchondral trabecular bone (Batiste *et al*., 2004; Wang *et al*., 2010; Li *et a*l., 2013). Characteristics of later stages are elevated apparent density, increased bone volume, thickening of subchondral bone plate, increased trabecular thickness, decrease of trabecular separation and bone marrow spacing, and transformation of trabeculae from rod-like into plate-like (Ding, 2010).

In this study, the result revealed that development of osteoarthritis in MIA group is slower than ACLT group because bone loss in femur still occurs even in week 12 which was supported by Liu *et al*. in 2016. Batiste *et al*. suggested that there will be loss of subchondral bone in the early stages of OA but as disease progress there will be increase stiffening of sclerotic subchondral bone. Both induction method shows increases of percent bone volume (BV/TV) the lateral condyle suggest that bone sclerosis had occurred while medial condyle still in bone loss stage. Therefore, development of OA in medial condyle is slower than lateral condyle of femur.

BV/TV of ACLT group in both medial and lateral condyles of tibia shows decrease from control to week 8 due to bone loss and bone remodelling. Medial

condyle of MIA group shows sclerosis without osteoporosis as development of OA can occur on day 15 post MIA injection supported by Mohan *et al*. in 2011. Sclerosis of medial condyle occurs faster in tibia than femur whereas sclerosis of lateral condyle occurs faster in femur than tibia. This can be due to limitation of this study as articular cartilage changes are not included in this study as Batiste *et al*., 2004 stated cartilage damage strongly related to thinning and increased porosity of the subchondral bone plate. Besides, medial condyle in tibia developed osteoarthritis faster probably due to thinning of the cartilage in medial condyle which caused biomechanical force distributed directly to the subchondral bone in medial compartment of tibia. Sclerosis occurred faster in the lateral condyle of femur due to more weight bearing on lateral in rabbit stated by Gushue *et al.,* 2005. More weight bearing on lateral caused more wears and tears on the lateral articular cartilage which in turned leads to changes in the lateral condyle of femur.

Florea *et al*. in 2014 stated that femur shows more changes in subchondral bone than tibia during development of osteoarthritis which supported the results shown in bone surface density. Bone surface density in femur showed normal development of osteoarthritis where bone remodelling occurred in early stage of osteoarthritis then followed by bone sclerosis in later stage which supported by Donell in 2019 in human journal. Thus, following the results shown animal model also have bone remodelling in the initial stage and then develop into sclerotic bone in later stage.

Bone surface density in tibia increased from control to week 4 due to fast development of OA. MIA in tibia has faster development of OA as the parameter of

bone surface density increase in week 4 as compared to ACLT group. Development of OA is much faster in lateral condyle of femur and medial condyle of tibia for MIA group. This is concurrent with the result in percent bone volume. Human cartilage of femur is thinner than cartilage in tibia. In normal circumstances, cartilage functions to lower friction during joint movement, absorbs the biomechanical forces, and stabilizes the joint (Moore, n.d) to prevent damage on the bone. Loss of cartilage will caused biomechanical forces directly applied on subchondral bone causing damage to subchondral bone. Due to the limitation of this study where articular cartilage was not measures and analyses in this case, the reasons of development of OA faster in lateral condyle of femur and medial condyle of tibia cannot be explained.

Trabecular thickness in femur for ACLT group shows increase in week 4 indicates bone sclerosis in late stage. Trabecular thickness in MIA group only increase in week 8 indicates that MIA induced OA slower than ACLT. Little & Smith in 2008 reported that ACLT induced OA more rapid than MIA. ACLT cause more joint instability which induce cartilage degeneration, subchondral bone sclerosis and osteophytes formation rapidly (Takahashi *et al*., 2018) while MIA requires a longer period of time as it cause the degeneration of articular cartilage and slowly leads to OA (Liu *et al*., 2016).Trabecular thickness in tibia shows the same result as femur where ACLT induced OA more rapid than MIA as bone sclerosis occurred in week 12 for ACLT but not MIA.

Normally, trabecular separation will decreases as trabecular thickness increases but in this case trabecular separation in ACLT femur increase while trabecular thickness increases indicates trabeculae number was low in week 4 for

early stage OA then it decreases in week 8 and increase afterward. Trabecular separation in MIA femur decrease in week 4 and increase in week 8 indicates bone remodelling occurred.

Trabecular separation and trabecular thickness of ACLT tibia shows decrease in week 4 with increase percent bone volume indicates that bone remodelling occurred in this stage where there is many thin trabecular formation results in short separation and high bone volume.

Only percent bone volume shows statistical significant in four variables: bone (femur and tibia), induction method of OA (control, ACLT and MIA), different point of time (week 4, 8, 12) and medial and lateral condyles. Bone surface density shows statistical significant in bone (femur and tibia) and different point of time. Trabecular thickness only shows statistical significant in bone (femur and tibia). Trabecular separation shows statistical significant in bone (femur and tibia) and induction method of OA (control, ACLT and MIA).

Medial and lateral condyles are statistical significant from each other. There are differences between weight bearing in rabbit and human. Rabbit bears weight more on the lateral compartment of the femorotibial joint whereas human bear weight more on medial compartment bears thus lateral condyle weight bearing has correlated with the presence of lateral conydle OA in femur. Rabbit weight distributed to four legs while human weight distributed to two legs. Hind limb bears more weight than forelimb in rabbit.

ACLT is statistical significant different from MIA. This is because MIA induced OA through inhibition of glyceraldehyde-3-phosphate dehydrogenase activity which leads to inhibition of glycolysis and induced chondrocytes death. While ACLT causes joint instability which leads to cartilage degeneration, subchondral bone sclerosis and osteophytes formation. MIA mimic naturally occur OA while ACLT mimic traumatic injury to the joint. Development of OA in ACLT is faster than MIA, thus MIA mimic age related OA while ACLT mimic traumatic OA.

6.0 Conclusion

The mechanisms of OA development in both induction methods are different. Bone remodeling has occurred in both methods. Each method has its own progression in developing OA. ACLT induction method has faster progression of OA as compared to MIA induction method. Femur and tibia have different development of OA. The changes in subchondral bone are different at different point of time (week 4, 8 and 12). First, there will be bone reabsorption by osteoclast followed by bone formation by osteoblast and lastly mineralization attenuated with bone stiffening in late phase. The changes in subchondral bone are different in medial and lateral condyles of femur and tibia. In ACLT induction method, more changes can be seen in medial condyle while in MIA induction method, more changes can be seen in lateral condyle.

7.0 Recommendations

The bone parameters investigated in this study provide a general idea of how OA occurred. There are lacking of a few assessment to well differentiate between ACLT and MIA such as pain assessment, macroscopic lesions, histopathology and biomarker for inflammation. Besides, relationship of the changes in articular cartilage and subchondral bone at different point of time should be done as articular cartilage changes could affect the changes in subchondral bone.

References

Aigner T, Schmitz N. Pathogenesis and pathology of osteoarthritis, In:Hochberg M, Silman A, Smolen J, Weinblatt M, Weisman M eds Rheumatology 5th edition, 2011, Philadelphia, Mosby Elsevier, 1741-1759.

Altman RD. Criteria for classification of clinical osteoarthritis. J Rheumatol.1991;18 SUPPL 27:10–2.

Altman R, Asch E, Bloch D, Bole G, Borenstein D, Brandt K, et al. Development of criteria for the classification and reporting of osteoarthritis: classification of osteoarthritis of the knee. Arthritis Rheum. 1986;29(8):1039– 49.

Athanasiou, K. A., Rosenwasser, M. P., Buckwalter, J. A., Malinin, T. I., & Mow, V. C. (1991). Interspecies comparisons of in situ intrinsic mechanical properties of distal femoral cartilage. Journal of Orthopaedic Research, 9(3), 330-340. doi:10.1002/jor.1100090304

Batiste DL, Kirkley A, Laverty S, Thain LM, Spouge AR, Holdsworth DW: Ex vivo characterization of articular cartilage and bone lesions in a rabbit ACL transection model of osteoarthritis using MRI and micro-CT. Osteoarthritis Cartilage 2004, 12:986–996.

Bouxsein, M. L., Boyd, S. K., Christiansen, B. A., Guldberg, R. E., Jepsen, K. J., & Müller, R. (2010).

Bove SE, Calcaterra SL, Brooker RM, Huber CM, Guzman RE, Juneau PL, et al. Weight bearing as a measure of disease progression and efficacy of anti-inflammatory compounds in a model of monosodium iodoacetate-induced osteoarthritis. Osteoarthritis Cartilage. 2003;11: 821–830. pmid:14609535

Buckwalter JA, Mankin HJ. Articular cartilage, part 1: tissue design and chondrocyte-matrix interaction. J Bone Joint Surg Am. 1997;79:600-611.

Chen, D., Shen, J., Zhao, W., Wang, T., Han, L., Hamilton, J. L., & Im, H. (2017). Osteoarthritis: Toward a comprehensive understanding of pathological mechanism. Bone Research, 5(1). doi:10.1038/boneres.2016.44

Cucchiarini, M., de Girolamo, L., Filardo, G., Oliveira, J. M., Orth, P., Pape, D., & Reboul, P. (2016). Basic science of osteoarthritis. Journal of experimental orthopaedics, 3(1), 22. https://doi.org/10.1186/s40634-016-0060-6

Danila, M. (2014). Biology of Normal Joint and Evaluation of the Joint Including Clinical, Imaging, and Pathologic Evaluation. Pathobiology of Human Disease, 1912-1919. doi:10.1016/b978-0-12-386456-7.04301-x

Ding M: Microarchitectural adaptations in aging and osteoarthritic subchondral bone issues. Acta Orthop Suppl 2010, 81:1–53

Durr HD, Martin H, Pellengahr C, Schlemmer M, Maier M, Jansson V: The cause of subchondral bone cysts in osteoarthrosis: a finite element analysis. Acta Orthop Scand 2004, 75:554–558.

Fernihough J, Gentry C, Malcangio M, Fox A, Rediske J, Pellas T, et al. Pain related behaviour in two models of osteoarthritis in the rat knee. Pain. 2004;112(1–2):83–93.

Ferrucci L, Cavazzini C, Corsi A, et al. Biomarkers of frailty in older persons. Journal of endocrinological investigation. 2002;25:10–15.

Florea, C., Malo, M., Rautiainen, J., Mäkelä, J., Fick, J., Nieminen, M., Korhonen, R. (2015). Alterations in subchondral bone plate, trabecular bone and articular cartilage properties of rabbit femoral condyles at 4 weeks after anterior cruciate ligament transection. Osteoarthritis and Cartilage, 23(3), 414-422. doi:10.1016/j.joca.2014.11.023

Garnero P, Peterfy C, Zaim S, Schoenharting M: Bone marrow abnormalities on magnetic resonance imaging are associated with type II collagen degradation in knee osteoarthritis: a three-month longitudinal study. Arthritis Rheum 2005, 52:2822–2829.

Goldring M, Goldring S: Articular cartilage and subchondral bone in the pathogenesis of osteoarthritis. Ann NY Acad Sci 2010, 1192:230–237.

Gregory MH, Capito N, Kuroki K, Stoker AM, Cook JL, Sherman SL. A review of translational animal models for knee osteoarthritis. Arthritis. 2012;2012:764621. doi:10.1155/2012/764621

Guingamp C, Gegout-Pottie P, Philippe L, Terlain B, Netter P, Gillet P. Monoiodoacetate- induced experimental osteoarthritis. A dose-response study of loss of mobility, morphology, and biochemistry. Arthritis Rheum. 1997;40(9):1670–9.

Gushue, D. L., Houck, J., & Lerner, A. L. (2005). Rabbit knee joint biomechanics: Motion analysis and modeling of forces during hopping. Journal of Orthopaedic Research, 23(4), 735-742. doi:10.1016/j.orthres.2005.01.005

Herzog W, Diet S, Suter E, Mayzus P, Leonard TR, Müller C, et al. Material and functional properties of articular cartilage and patellofemoral contact mechanics in an experimental model of osteoarthritis. J Biomech 1998;31:1137e45.

Holdsworth, D. and Thornton, M., 2002. Micro-CT in small animal and specimen imaging. Trends in Biotechnology, 20(8), pp.S34-S39.

Holmdahl DE, Ingelmark BE: The contact between the articular cartilage and the medullary cavities of the bone. Acta Orthop Scand 1950, 20:156–165.

Intema F, Hazewinkel HA, Gouwens D, Bijlsma JW, Weinans H, Lafeber FP, Mastbergen SC: In early OA, thinning of the subchondral plate is directly related to cartilage damage: results from a canine ACLT-meniscectomy model. Osteoarthritis Cartilage 2010, 18:691–698.

International, O. R. (2016). Osteoarthritis: A Serious Disease, Submitted to the US Food and Drug Administration, 1-103.

Johnson, F., Leitl, S., & Waugh, W. (1980). The distribution of load across the knee. A comparison of static and dynamic measurements. The Journal of Bone and Joint Surgery. British Volume, 62-B(3), 346-349. doi:10.1302/0301-620x.62b3.7410467

Judex S, Gross TS, Bray RC, Zernicke RF. Adaptation of bone to physiological stimuli. J Biomech 1997;30:421e9.

Kim JE, Song D-h, Kim SH, Jung Y, Kim SJ (2018) Development and characterization of various osteoarthritis models for tissue engineering. PLoS ONE 13(3): e0194288. https://doi.org/10.1371/journal.pone.0194288

Kuyinu, E. L., Narayanan, G., Nair, L. S., & Laurencin, C. T. (2016). Animal models of osteoarthritis: Classification, update, and measurement of outcomes. Journal of Orthopaedic Surgery and Research, 11(1). doi:10.1186/s13018-016-0346-5

Laverty, C. A. Girard, J. M. Williams, E. B. Hunziker, and K. P. H. Pritzker, "The OARSI histopathology initiative— recommendations for histological assessments of osteoarthritis in the rabbit," Osteoarthritis and Cartilage, vol. 18, supplement 3, pp. S53–S65, 2010.

Li et al.: Subchondral bone in osteoarthritis: insight into risk factors and microstructural changes. Arthritis Research & Therapy 2013, 15:223

Li, G., Yin, J., Gao, J., Cheng, T. S., Pavlos, N. J., Zhang, C., & Zheng, M. H. (2013). Subchondral bone in osteoarthritis: Insight into risk factors and microstructural changes. Arthritis Research & Therapy, 15(6), 223. doi:10.1186/ar4405

Little, C., & Smith, M. (2008). Animal Models of Osteoarthritis. Current Rheumatology Reviews, 4(3), 175-182. doi:10.2174/157339708785133523

Liu, Z., Hu, X., Man, Z., Zhang, J., Jiang, Y., & Ao, Y. (2016). A novel rabbit model of early osteoarthritis exhibits gradual cartilage degeneration after medial collateral ligament transection outside the joint capsule. Scientific Reports, 6(1). doi:10.1038/srep34423

Loeser, R. F., Goldring, S. R., Scanzello, C. R., & Goldring, M. B. (2012). Osteoarthritis: A disease of the joint as an organ. Arthritis & Rheumatism, 64(6), 1697-1707. doi:10.1002/art.34453

Lorensen W, Cline H. Marching cubes: a high resolution 3D surface construction algorithm. Computer Graphics. 1987;21:163–169.

Madry H, van Dijk CN, Mueller-Gerbl M: The basic science of the subchondral bone. Knee Surg Sports Traumatol Arthrosc 2010, 18:419–433.

Man, G. S., & Mologhianu, G. (2014). Osteoarthritis pathogenesis - a complex process that involves the entire joint. Journal of medicine and life, 7(1), 37–41.

Mansell JP, Bailey AJ: Abnormal cancellous bone collagen metabolism in osteoarthritis. J Clin Invest 1998, 101:1596–1603

Marker CL, Pomonis JD. The monosodium iodoacetate model of osteoarthritis pain in the rat. Methods Mol Biol. 2012;851:239–48.

Mark Edwards, Anna Litwic, Elaine Dennison, & Cyrus Copper. (2013). Epidermiology and Burden of Osteoarthritis. Br Med Bull, 185-199.

Martel-Pelletier, J., Lajeunesse, D., Reboul, P., & Pelletier, J. (2007). The Role of Subchondral Bone in Osteoarthritis. Osteoarthritis, 15-32. doi:10.1016/b978-0-323-03929-1.50007-0

Matsui H, Shimizu M, Tsuji H. Cartilage and subchondral bone interaction in osteoarthrosis of human knee joint: a histological and histomorphometric study. Microsc Res Tech 1997;37: 333e42.

McCoy AM (2015) Animal models of osteoarthritis: comparisons and key considerations. Vet Pathol 52:803–818

Mitchell RE, Huitema LFA, Skinner REH, Brunt LH, Severn C, Schulte-Merker S, Hammond CL (2013) New tools for studying osteoarthritis genetics in zebrafish. Ostearthr Cartil 21(2):269–278

Mohamed Ali Rebai, Nizar Sahnoun, Oussema Abdelhedi, Khaled Keskes, Slim Charfi, Fathia Slimi, Rim Frikha & Hassib Keskes (2020) Animal models of osteoarthritis: characterization of a model induced by Mono-Iodo-Acetate injected in rabbits, Libyan Journal of Medicine, 15:1, 1753943, DOI: 10.1080/19932820.2020.1753943

Moore, D. (n.d.). Articular Cartilage. Retrieved August 17, 2020, from https://www.orthobullets.com/basic-science/9017/articular-cartilage

Mow VC, Yong Gu W, Hui Chen F. Structure and function of articular carilage and meniscus, In Mow VC, Huiskers R eds, Basic Orthopaedic Biomechanics and Mechano-Biology 3rd Edition, 2005, Philadelphia, Lippincot Williams & Wilkins, 181-258

Muller R, Ruegsegger P. Three-dimensional finite element modelling of non-invasively assessed trabecular bone structures. Med Eng Phys. 1995;17:126–133.

Nigg BM, Herzog W. Joints. In: Biomechanics of the Musculoskeletal System. 3rd edn. Chichester, West Sussex, England: Ed. John Wiley & Sons; 2007:244e91.

Ondrouch AS: Cyst formation in osteoarthritis. J Bone Joint Surg Br 1963, 45:755

OpenStax. (2013, March 06). 9.6 Anatomy of Selected Synovial Joints. Retrieved August 10, 2020, from https://opentextbc.ca/anatomyandphysiology/chapter/9-6-anatomy-of-selected-synovial-joints/

Pan J, Zhou X, Li W, Novotny JE, Doty SB, Wang L: In situ measurement of transport between subchondral bone and articular cartilage. J Orthop Res 2009, 27:1347–1352 Peters ST, Wilke M, Schmid T. Arthroscopic approach and anatomy of the stifle joint in the rabbit. Veterinary Surgery. 2018;47:130-135. https://doi.org/10.1111/vsu.12727

Parfitt A, Drezner M, Glorieux F, Kanis J, Recker R. Bone histomorphometry: standardization of nomenclature, symbols and units. J Bone Miner Res. 1987;2:595–610.

Pelletier J, Boileau C, Altman RD, Martel-Pelletier J. Experimental models of osteoarthritis: usefulness in the development of disease-modifying osteoarthritis drugs/agents. Therapy. 2010;7(6):621–34.

Radin EL, Rose RM. Role of subchondral bone in the initiation and progression of cartilage damage. Clin Orthop Relat Res. 1986 Dec;(213):34-40. PMID: 3780104.

Samvelyan, H.J., Hughes, D., Stevens, C. et al. Models of Osteoarthritis: Relevance and New Insights. Calcif Tissue Int (2020). https://doi.org/10.1007/s00223-020-00670-x

Senin (2019, December 23). Labeled Simple Knee Joint Diagram. Retrieved August 17, 2020, from https://myflyingboxandme.blogspot.com/2019/12/labeled-simple-knee-joint-diagram.html

Shane Anderson, A., & Loeser, R. F. (2010). Why is osteoarthritis an age-related disease?. Best practice & research. Clinical rheumatology, 24(1), 15–26. https://doi.org/10.1016/j.berh.2009.08.006

Shimizu M, Tsuji H, Matsui H, Katoh Y, Sano A. Morphometric analysis of subchondral bone of the tibial condyle in osteoarthrosis. Clin Orthop Relat Res 1993;293:229e39.S.

Teeple E, Jay GD, Elsaid KA, Fleming BC (2013) Animal models of osteoarthritis: Challenges of model selection and analysis. AAPS J 15:438–446

T. Muraoka, H. Hagino, T. Okano, M. Enokida, and R. Teshima, "Role of subchondral bone in osteoarthritis development: a comparative study of two strains of guinea pigs with and without spontaneously occurring osteoarthritis," Arthritis & Rheumatism, vol. 56, no. 10, pp. 3366–3374, 2007.

Wang Y, Wluka AE, Pelletier JP, Martel-Pelletier J, Abram F, Ding C, Cicuttini FM: Meniscal extrusion predicts increases in subchondral bone marrow lesions and bone cysts and expansion of subchondral bone in osteoarthritic knees. Rheumatology (Oxford) 2010, 49:997–1004.

Wise C. Osteoarthritis, In Dale DC, Federman DD eds, ACP Medicine section 15, chap. 10, 2010, New York, WebMD, 1-12.

Yoneda T. Cytokines in bone: local translators in cell-to-cell communications. In: Cellular and Molecular Biology of Bone. 1st edn. San Diego: Ed. Academic Press Limited; 1993: 375e412.